

SUPPLEMENTAL MATERIAL

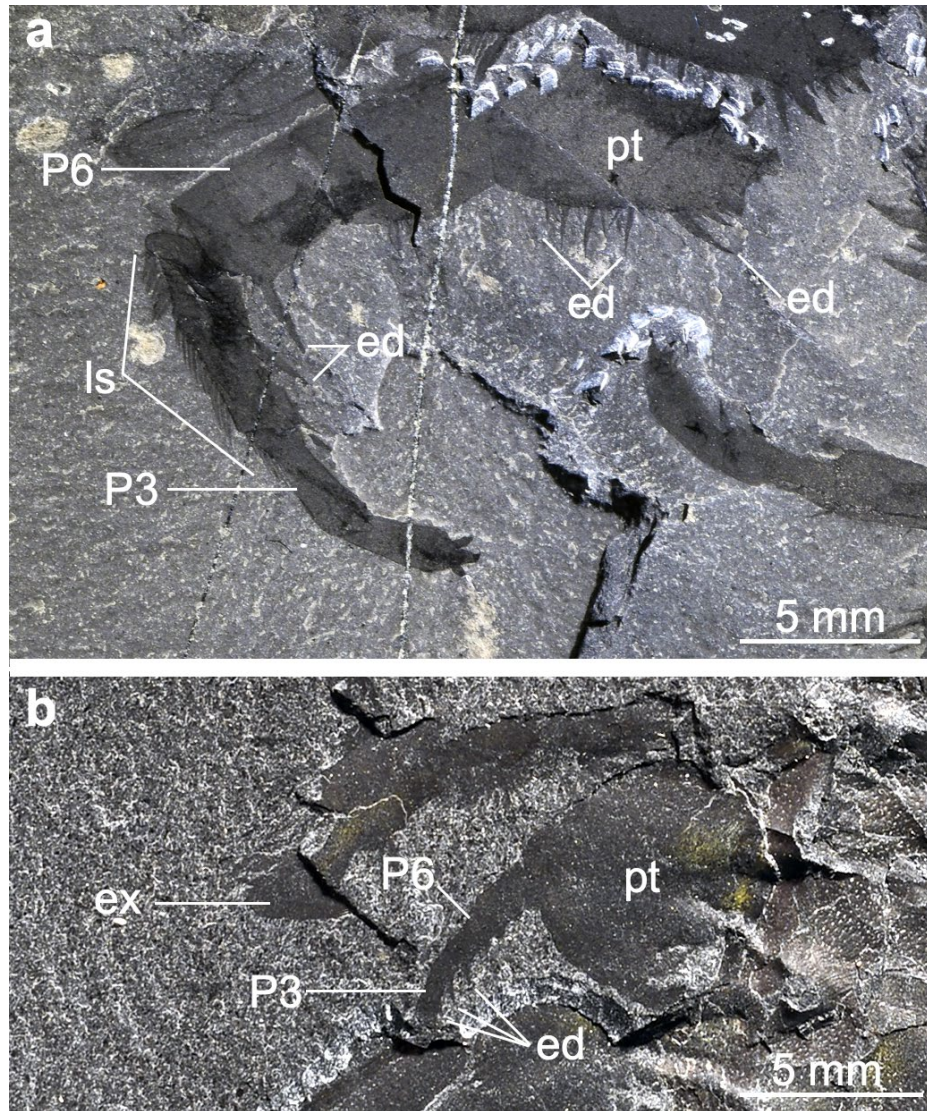


Figure S1. Comparison between conventional biramous trunk appendages and modified claspers in *Olenoides serratus* from the Cambrian (Wuliuan) Burgess Shale. a, GSC 34692 appendage nine photographed under cross polarized light. B, ROMIP 66299 appendage 10 photographed under cross polarized light. Abbreviations: ed, endite; ex, exopodite; ls, lateral setae; pn, podomere number; pt, protopodite.

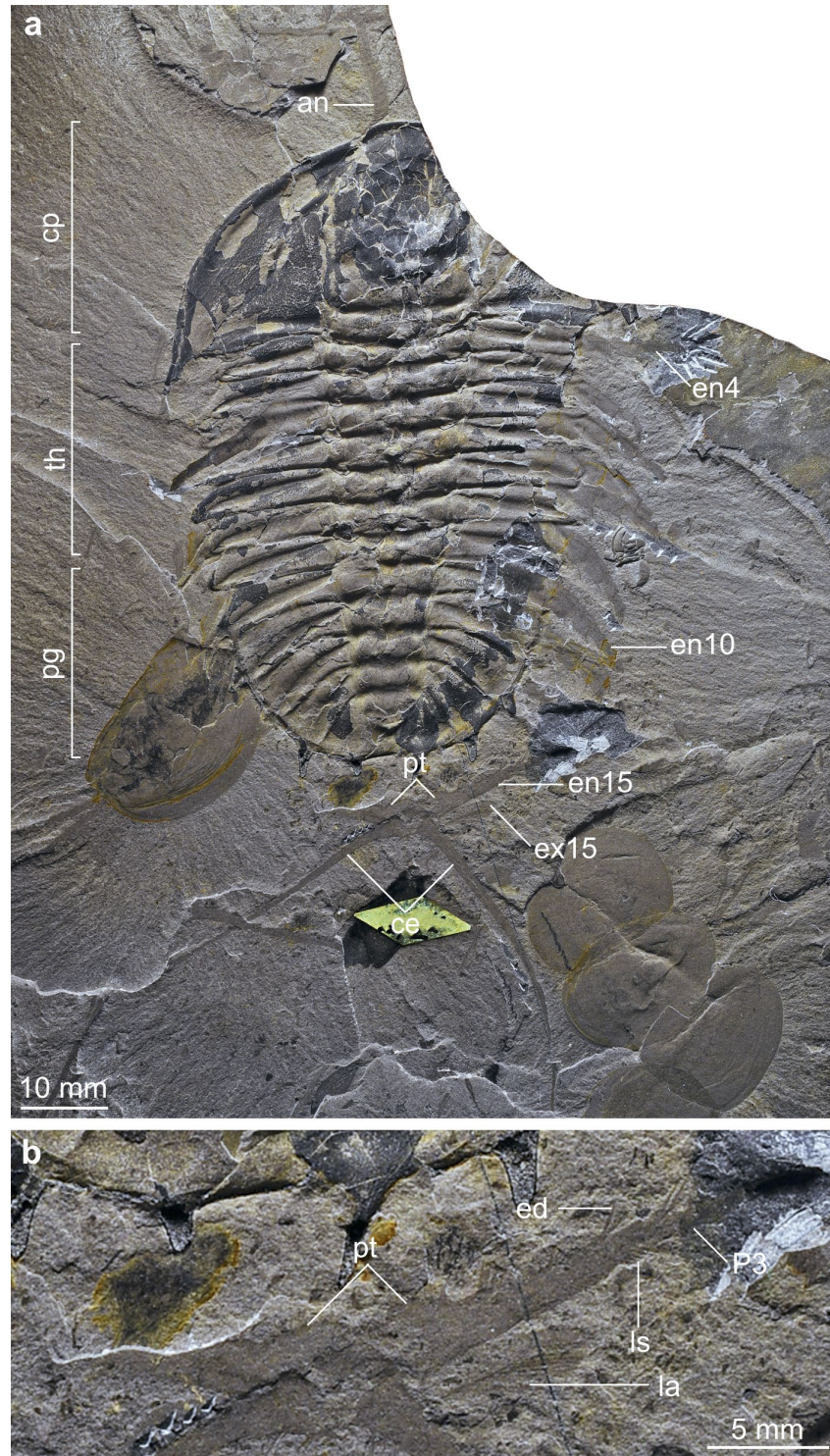


Figure S2. *Olenoides serratus* with preserved appendages. a, Dorsal view of USNM 57656 with antenna, nine endopodites, and cerci preserved photographed under cross polarized light. b, Magnification of fifteenth appendage pair photographed under cross polarized light. Abbreviations: an, antenna; ce, cerci; en*n*, endopodite number; ex, exopodite; pg, pygidium; P*n*, podomere number; pt, protopodite; th, thorax.

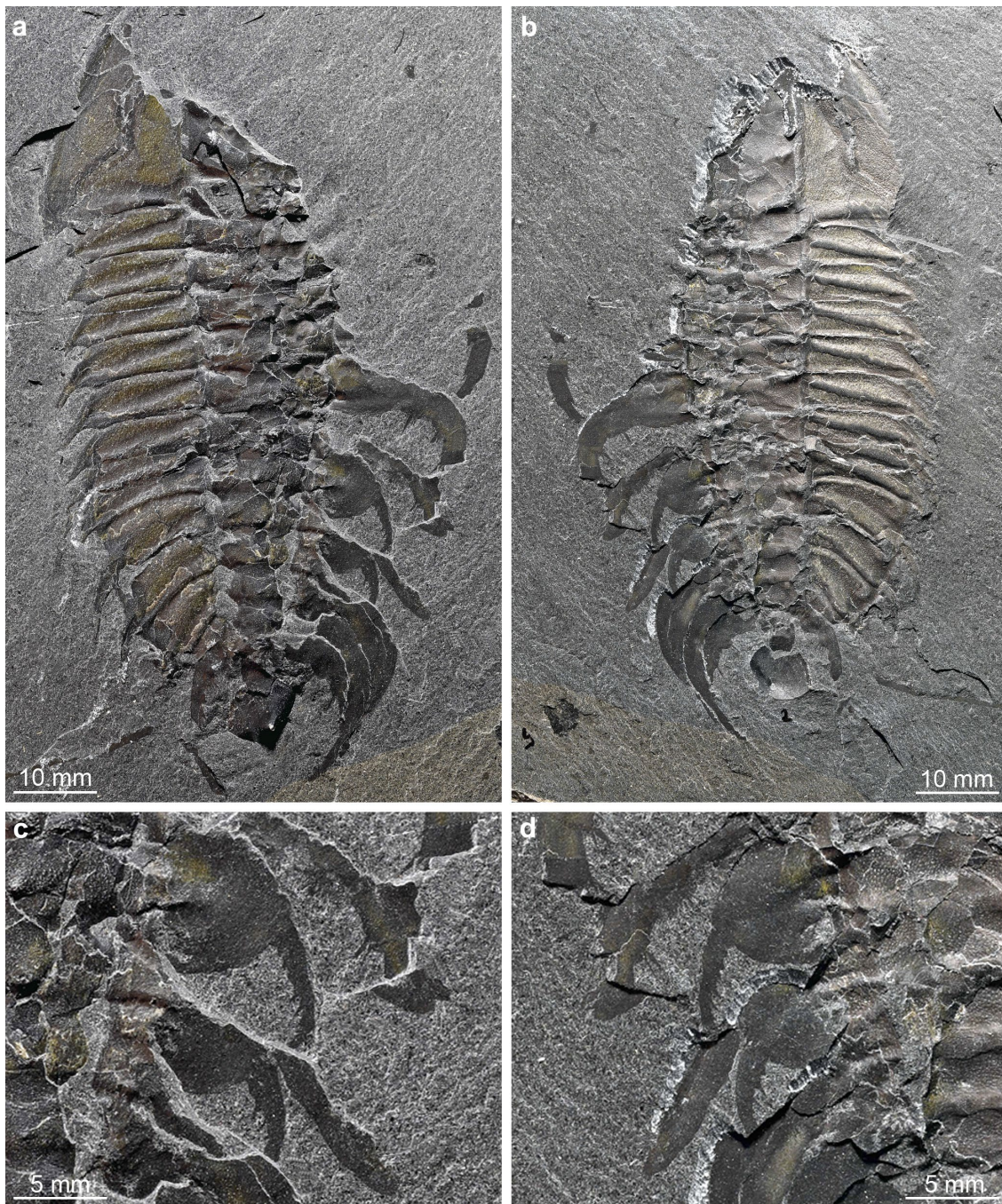


Figure S3. Claspers in *Olenoides serratus* from the Cambrian (Wuliuan) Burgess Shale. a,b, ROMIP 66299, part and counterpart photographed under cross polarized light without annotations. c,d, Details of tenth and eleventh appendages photographed under cross polarized light without annotations.

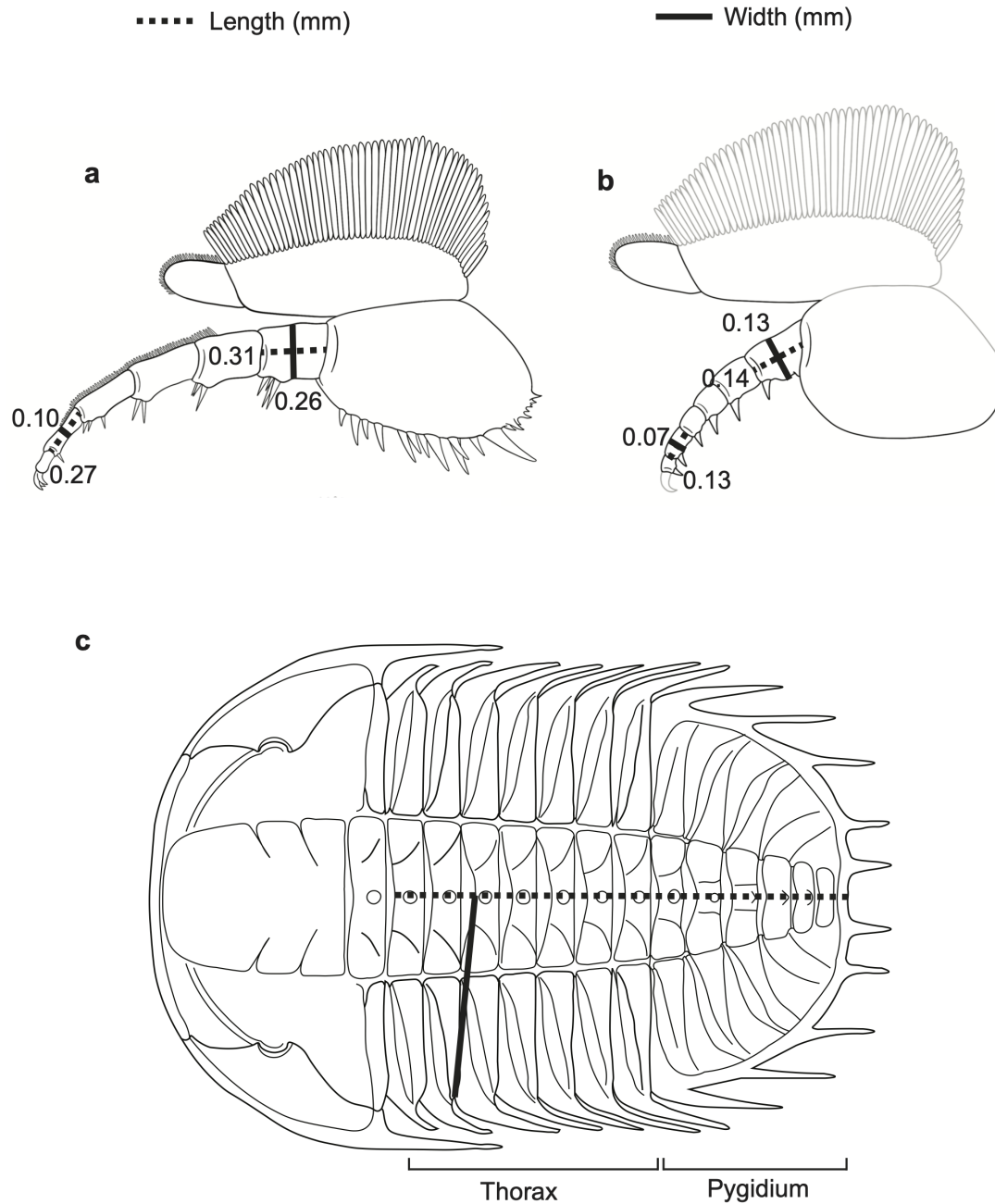


Figure S4. Measurements in *Olenoides serratus* from the Cambrian (Wuliuan) Burgess Shale. a, Length and width measurements of podomeres in normal endopodite. b, Length and width measurements of podomeres from claspers. c, Measurements of thorax length, pygidium length, and width at third tergite without pleural spine used as estimated for body size.

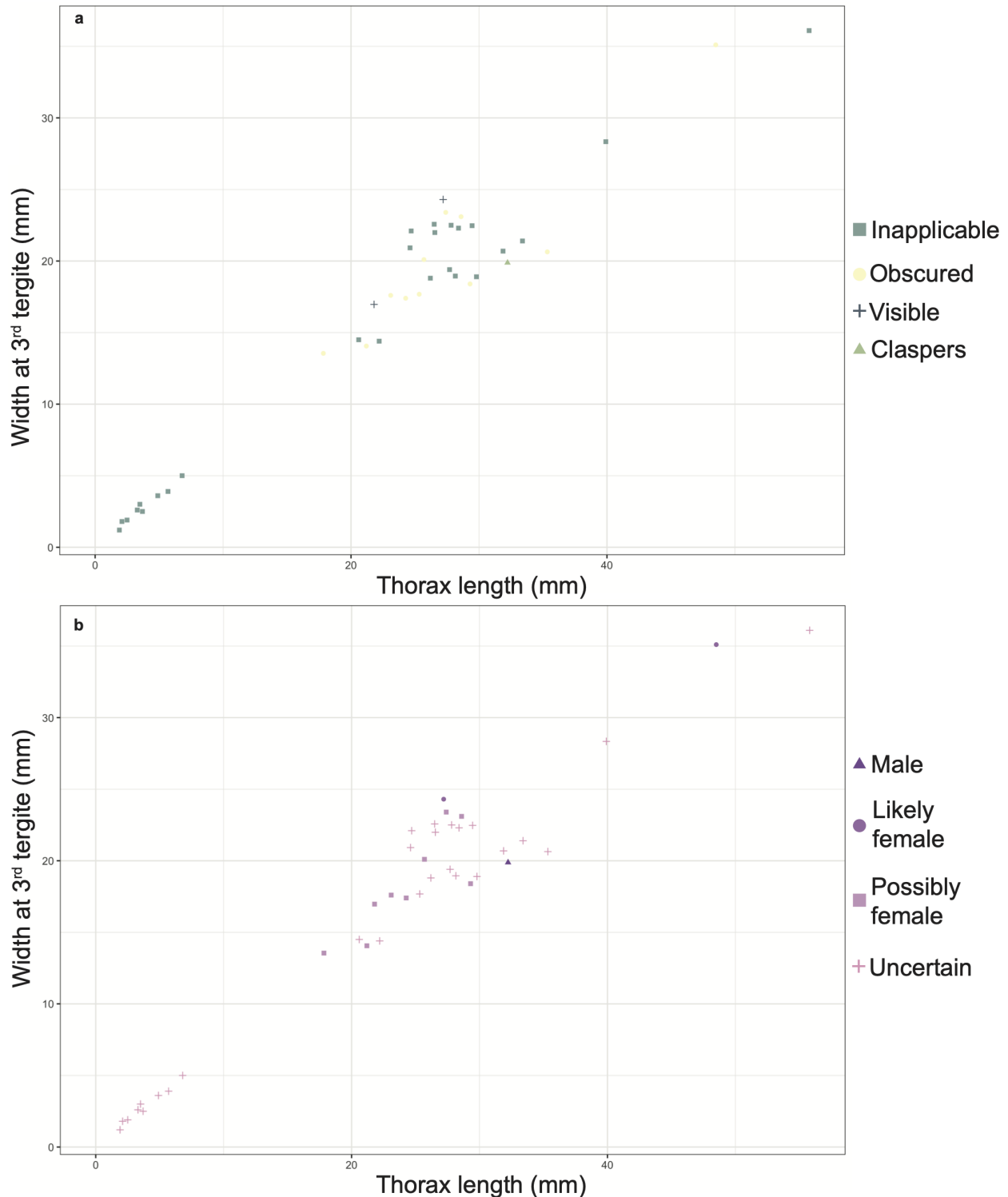


Figure S5. *Olenoides serratus* specimen size. Specimens were measured as shown in Figure S4c. Size data available in Supplementary Table 3. a, Specimens color coded by presence of endopodites 10 and or 11. Inapplicable for specimens that do not have endopodite 10 and or 11. Obscured for specimens with exoskeleton that would cover claspers. Visible for specimens with entire endopodite exposed. Clasper for specimens with entire reduced endopodite exposed. b, Specimens color coded by likely sex. Male identified by the presence of claspers. Likely females

include specimens with endopodites 10 and or 11 (obscured or visible) and large in size. Possibly females are specimens with endopodites 10 and or 11 (obscured or visible) but smaller than ROM IP66299 or unmeasurable. Uncertain for specimens without endopodites 10 and or 11 preserved.

Supplemental Discussion

Appendage specialization in artiopods.

Artiopods are a clade of crown-group euarthropods that were a significant component of the Paleozoic oceans and include the extremely abundant trilobites, which are well represented in the fossil record thanks to their biomineralized calcitic dorsal exoskeleton (Wilmot, 1989). Although artiopods have been traditionally considered to bear predominantly homonomous appendages (Hou and Bergström, 1997; Wills et al., 1998; Zeng et al., 2017), recent work has shown a greater degree of differentiation than originally thought in several non-biomineralized representatives (Schmidt et al., 2022). For example, the xandarellid *Sinoburius lunaris* shows a specialization the first three appendage pairs, having a modified set of antennae and stenopodous exopodites on the first and second post-antennal appendages with greatly reduced endopodites (Chen et al., 2019; Schmidt et al., 2022). Another non-trilobite artiopod from Chengjiang, *Pygmaclypeatus daziensis*, shows four morphologically distinct sets of biramous appendages, which vary in terms of the size and shape of the exopodite, presence of spinose endites, and even the differentiation of the terminal claws on the endopodites (Schmidt et al., 2022). Endite morphology and density on the protopodite of the nektaspid *Naraoia spinosa* has also been shown to change throughout ontogeny, with different ecological and feeding implications for juveniles and adults (Zhai et al., 2019).

Despite the existence of over 20,000 described species of trilobites, details of their ventral non-biomineralized anatomy are only preserved in 38 taxa reported to date (Supplementary Table 1). Trilobites with preserved appendages feature a pair of uniramous antennae followed by a homonomous series of biramous appendages, typically with three underneath the cephalon and one per tergite in the trunk, although with a seemingly widespread pattern of dorsoventral segmental mismatch (Ortega-Hernández and Brena, 2012). All the biramous appendages have similar morphology, and the main evidence of differentiation consists of the presence of progressively smaller posterior limb pairs (Siveter et al., 2021). One species, *Redlichia rex*, exhibits moderate alterations in exopodite proportions along the body axis (Holmes et al., 2020). In two other species, *Eoredlichia intermedia* and *Triarthrus eatoni* the endite morphology on the protopodite changes from the anterior to posterior appendages (Holmes et al., 2020).

Biramous podomere morphology in *Olenoides serratus*.

The proximal podomeres of the endopodite have nearly square outlines, while distal more podomeres become elongate. P7 (podomere seven) is subquadrate, with a single endite almost equally long as the podomere is wide protruding from the middle of the ventral edge surrounded

by a cluster of smaller endites. P6 and P5 resemble each other, being subquadrate with a cluster of endites around a prominent pair near the distal edge. P5 is slightly more elongate distally, and has endites directly at the distal edge, as well as two small endites at the midpoint. P4 is rectangular with two large, distal endites that fork and two small endites in a row at the midpoint of the ventral edge. P3 is elongate with an hourglass shape that is narrowest in the middle, at least one endite protrudes distally, and is equally long as the podomere is wide at the midpoint. A line of lateral setae runs along the dorsal edge of P5-P3 (Supplementary Fig. 1a). The lateral setae are short and closely packed. The row of lateral setae is often disturbed during burial demonstrating the less rigid nature than the endites. P2 is club shaped with an inflated distal edge and a curved ventral margin lacking endites. P1 forms three claws that curve ventrally. The exopodite is composed of an elongate proximal lobe with long lamellae and a distal rounded lobe with shorter setae (Hou et al., 2021). The exopodite extends over P6 and the lamellae are anteriorly imbricated.

Variability of podomere morphology in *Olenoides serratus* endopodites.

The endopodites in appendages 10 and 11 are not only substantially smaller, but the individual podomeres have unique morphologies compared to the other appendages preserved on ROMIP 66299, and of other *Olenoides serratus* specimens (Fig. 3b). The protopodites of appendages 10 and 11 are shorter along the axis of the ramus than that of eight, with a rounder outline and noticeable lack of endites, which are visible on most other protopodites preserved in posterior or anterior views (Fig. 3b). By contrast, all other specimens of *O. serratus* with preserved subtriangular protopodites feature endites forming a gnathobase along the medial edge, a prominent large and robust spine at the ventral-medial inflection point, and ventromedially directed spines continuing along the ventral edge (Fig. 2a).

P7 shows slight variability in shape, from subquadrate to rectangular, but all podomeres measured fall along a single trend line, except for ROMIP 66299 endopodites 10 and 11 which are squarer (Fig. 3c). Measured P6 generally fall in a triangular morphospace, with most being longer than wide although a few are slightly wider than long. P6 shows more variability than P7, yet both ROMIP 66299 endopodite 10 and 11 do not fall within the same morphospace as all other podomeres (Fig. 3c). P5 and P4 show similar trends as P6, with most podomeres forming a cluster along a 1:1 ration, but with ROMIP 66299 endopodites 10 and 11 being substantially smaller (Fig. 3c). P3 shows a rectangular shape for most podomeres and a more contracted morphospace displaying less variability in shape. Although ROMIP 66299 endopodite 10 is the shortest of all measured P3, multiple other specimens have appendages with similarly wide P3 (Fig. 3c). P2 resembles P3, with a tightly clustered group of rectangular podomeres (Fig. 3c). For both podomeres ROMIP 66299 endopodite 10 is the smallest, although other specimens have similarly sized podomeres (Fig. 3c; Supplementary Table 2). P3 and P4 usually develop hourglass or club shapes (Fig. 2a), making them narrow at the midpoint, which could artificially make the reduced endopodites similar despite the obvious differences in morphology.

Endopodite eight from ROMIP 66299 has two measurable podomeres (Fig. 3c), both of which fall near the center of their respective clusters. ROMIP 66299 endopodite eight P6 is nearly

three times as long as endopodites 10 and 11, although it is only twice as wide. Specimen GSC 34694 is of a similar size (40.6 mm long from thorax to pygidium) and has preserved appendages in the same position as the reduced endopodites of ROMIP 66299, allowing for comparison. All podomeres in endopodite 10 of GSC 34694 cluster with other non-reduced appendages (Fig. 3c). The reduced endopodites are substantially shorter and narrower than even the smallest appendages found on other specimens, which are located at the posterior of the pygidium. Even these appendages, such as USNM 58589 endopodite 13 (Fig. 3b), show substantial morphological differences from the reduced endopodites of ROMIP 66299, notably the hourglass shape of P3, which is fully developed despite the small size. The endopodites of limb pair 15 from USNM 57656 (Supplementary Figure 1, Table 2) are more similar in size to the reduced endopodites of ROMIP 66299. The protopodites of the former are truncated ventrally because of the angle of burial, making them appear short and more rounded (Supplementary Figure 1b), yet ventral endites are still visible. Although endopodite 15 of USNM 57656 is small in overall size, all the podomeres are both longer and wider than those seen in endopodites 10 and 11 of ROMIP 66299 (Supplementary Table 2). The endopodite 15 of USNM 57656 also features well-developed endites, lateral setae, and the distinctive hourglass shape of P3, attesting to its conventional organization for most *Olenoides serratus* appendages.

Is reparative regeneration an alternative interpretation?

Reparative regeneration is well known throughout metazoans (Maruzzo et al., 2005; Seifert et al., 2012) and the dorsal exoskeleton of trilobites has been shown to heal after damage (Pates et al., 2017) following the developmental identities of tergites with the oldest/anterior re-growing first (McNamara and Tuura, 2011). However, there are no confirmed cases of limb regeneration in trilobites. Regenerating appendages of extant euarthropods are small when first released from the limb stub (Bliss, 1960) growing and changing morphology with subsequent molts but with otherwise similar proportions to undamaged appendages (Maruzzo et al., 2005; Nakamura et al., 2008; Maruzzo and Bortolin, 2013). In ROMIP 66299, the entire endopodites of appendages 10 and 11 exhibit a unique morphology, indicating that if this is regeneration, the damage was extensive and occurred even on the most proximal podomeres. After severe damage appendages are often not able to completely regenerate, or only wound healing will occur if the injuries are too substantial (Rosin, 1964; Shaw and Bryant, 1974; Maruzzo and Bortolin, 2013). The reduced endopodites 10 and 11 of ROMIP 66299 could be examples of poor regeneration where an appendage is regrown but is not structurally functional (Maruzzo and Bortolin, 2013). Scorpions regenerate small appendages that are not fully functional and with different proportions of segments relative to non-damaged appendages (Rosin, 1964). Endopodites 10 and 11 may also be examples of effective regeneration, but soon after release from the limb stub before growing to a regular size with molts. Although either interpretation of endopodites 10 and 11 could explain the difference in size relative to other limbs in ROMIP 66299, this hypothesis is contradicted by the morphology of the appendages themselves. Based on comparison with extant analogues, regenerating appendages in trilobites would have the same proportions (e.g. subtriangular

protopodite) and functional morphology (e.g. spinose endites), albeit at a smaller scale; this is not the case in ROMIP 66299 (see Supplementary Fig. 2). Regenerating appendages begin forming in the limb stub, which can undergo morphological changes such as muscle degeneration (seen in cockroaches) and changes in setae patterns (seen in scorpions) (Maruzzo and Bortolin, 2013), but in other cases there are no external modifications to the proximal most portion of the limb (Nakamura et al., 2008). If the protopodite composed the entirety of the limb stub, with the endopodite regenerating within until release (Bliss, 1960; Maruzzo and Bortolin, 2013), it might account for the rounded shape and lack of endites. In cockroaches and scorpions, the segment proximal to the amputation can experience degeneration of muscles and changes in setal patterns (Bliss, 1960; Maruzzo and Bortolin, 2013). The unique podomere morphology also does not match the interpretation of regeneration. When cricket legs regenerate after damage all segments are released at once, and although they are substantially smaller than normal, the segments display similar relative proportions to undamaged limbs (Nakamura et al., 2008). The similar size of appendages 10 and 11 in ROMIP 66299 also argues against regeneration. Given the pattern of regeneration seen in the dorsal exoskeleton (McNamara and Tuura, 2011), it would be expected that the oldest appendage would regenerate first, and thus show a discrepancy in size between appendages 10 and 11.

Possible reproductive roles for reduced endopodites.

A possible reproductive role for the reduced endopodites of *Olenoides serratus* would fall into one of two categories; appendages for spermatophore transfer (i.e. gonopods) or to grasp females during mating (i.e. claspers) (Botton et al., 1996; Gerhart, 2007). Limbs specialized for reproduction are widespread among extant euarthropods. Male pycnogonids have an additional appendage used to carry eggs, known as the oviger (Poschmann and Dunlop, 2006) (Fig. 3k, l). Gonopods have convergently evolved in millipedes and pancrustaceans from appendages in different parts of the body, but all occur in adult males and are used to transfer sperm to the female (Boxshall, 2004). Gonopods of extant euarthropods may be reduced in size compared to the other appendages, and often have a highly modified functional morphology (Drago et al., 2011; Car and Harvey, 2013; Sigvardt and Olesen, 2014; Boudinot, 2018). The reduced endopodites in *O. serratus* do not resemble gonopods of other euarthropods as they lack clear modifications that would aid in direct spermatophore transfer such as sperm grooves (Fig. 3g).

Sexual dimorphism in trilobites.

The claspers of ROMIP 66299 provide clear evidence of sexually dimorphic morphology, but only expressed in the appendages of adult males. No clear differences in the exoskeleton are shown in ROMIP 66299. Although the absence of the complete cephalon in ROMIP 66299 makes it impossible to completely rule out some degree of exoskeletal differentiation in the head beyond question, we consider that this is extremely unlikely given the abundance of well preserved complete specimens, none of which show significant morphological variability in this regard.

Confident identification of sex would rely on preservation of endopodites 10 and 11, which are found in 23 specimens; however only in three (GSC 34294, GSC 74993-2, and ROM 000976) specimens show the entire endopodite exposed (Supplementary Table Claspers). Unlike normal sized appendages, the claspers would not be visible underneath the exoskeleton even in extremely well preserved specimens unless there was significant displacement away from the body, or a breakage in the dorsal exoskeleton (as observed in ROMIP 66299).

The timing for the metamorphosis of endopodites 10 and 11 into claspers is unknown but would likely occur upon reaching the holaspide phase at the onset of sexual maturity. Small juvenile (meraspide) males would likely retain the undifferentiated appendages, making them completely indistinguishable from females. USNM 273311 and GSC 34692 are possible females with endopodites 10 and 11 preserved as they are similar in size or larger than ROMIP 66299, but both the exoskeleton could obscure claspers if present (Supplementary Table 3). Although GSC 34294, GSC 74993-2, and ROM 000976 completely show endopodites 10 and 11, GSC 34294 is smaller than ROMIP 66299 and ROM 000976 couldn't be measured accurately because of damage to the exoskeleton. GSC 74993-2 is the most likely to be female since it is similar in size to ROMIP 66299 and clearly shows the entire endopodite with a normal morphology.

A previous study of potential sexual dimorphism in trilobites tentatively suggested size differences, with females being larger than males as commonly observed in living euarthropods (Hu, 1971). However, ROMIP 66299 is a large specimen, which implies that either there are no female specimens known of *Olenoides serratus* (*sensu* Hu, 1971), or males are not necessarily smaller than females. Without substantial evidence of size differentiation, we assume that amplexus in *O. serratus* would likely take place among individuals of a similar body size (Fig. 4).

Fortey and Hughes (1998) proposed sexual dimorphism in trilobites that relied on the easily fossilized dorsal exoskeleton, and in particular suggested that the inflated preglabellar fields were potentially used by females to brood fertilized eggs in many species of trilobites. *Olenoides serratus* clearly shows sexual dimorphism, but the morphological differences are only expressed in the ventral appendages, which rarely preserve. This would make identification of sex difficult for trilobites if this is true across the clade. The abundance and longevity of Trilobita makes it extremely likely that species utilized different breeding strategies, as seen with bivalved euarthropods with different numbers and sizes of egg clutches (Ou et al., 2020), trilobites with lecithotrophic embryos (Laibl et al., 2017), and brooding versus spawning strategies in decapods (Dall et al., 1990; Wanninger, 2015). Thus, we refrain from generalizing our conclusions on the sexual dimorphism seen in *O. serratus* to all other trilobites, particularly those species that are phylogenetically or spatiotemporally distant. We consider that there is a high likelihood that sexual dimorphism in trilobites would most likely have been expressed in numerous forms given the substantial diversity and longevity of these euarthropods, but further confirmation will likely necessitate the input of more material from Konservat-Lagerstätten which provide more detailed morphological information.

References

- Bliss, D.E., 1960, Autotomy and regeneration, in *The physiology of Crustacea*, New York, NY, Academy Press, v. 1, p. 561–589.
- Botton, M.L., Shuster, C.N., Sekiguchi, K., and Sugita, H., 1996, Amplexus and mating behavior in the Japanese horseshoe crab, *Tachypleus tridentatus*: *Zoological Science*, v. 13, p. 151–159, doi:10.2108/zsj.13.151.
- Boudinot, B.E., 2018, A general theory of genital homologies for the Hexapoda (Pancrustacea) derived from skeletomuscular correspondences, with emphasis on the Endopterygota: *Arthropod Structure & Development*, v. 47, p. 563–613, doi:10.1016/j.asd.2018.11.001.
- Boxshall, G.A., 2004, The evolution of arthropod limbs: *Biological Reviews*, v. 79, p. 253–300, doi:10.1017/S1464793103006274.
- Car, C., and Harvey, M., 2013, A review of the Western Australian keeled millipede genus *Boreoheperus* (Diplopoda, Polydesmida, Paradoxosomatidae): *ZooKeys*, v. 290, p. 1–19, doi:10.3897/zookeys.290.5114.
- Chen, X., Ortega-Hernández, J., Wolfe, J.M., Zhai, D., Hou, X., Chen, A., Mai, H., and Liu, Y., 2019, The appendicular morphology of *Sinoburius lunaris* and the evolution of the artiopodan clade Xandarellida (Euarthropoda, early Cambrian) from South China: *BMC Evolutionary Biology*, v. 19, p. 165, doi:10.1186/s12862-019-1491-3.
- Dall, W., Hill, B.J., Rothlisberg, P.C., and Sharples, D.J., 1990, Biology of the Penaeidae, in *Advances in Marine Biology*, London, Academic Press, v. 27.
- Drago, L., Fusco, G., Garollo, E., and Minelli, A., 2011, Structural aspects of leg-to-gonopod metamorphosis in male helminthomorph millipedes (Diplopoda): *Frontiers in Zoology*, v. 8, p. 19, doi:10.1186/1742-9994-8-19.
- Fortey, R.A., and Hughes, N.C., 1998, Brood Pouches in Trilobites: *Journal of Paleontology*, v. 72, p. 638–649.
- Gerhart, S.D., 2007, A review of the biology and management of horseshoe crabs, with emphasis on Florida populations: Fish and Wildlife Research Institute Technical Report TR-12. ii, p. 1–25.
- Holmes, J.D., Paterson, J.R., and García-Bellido, D.C., 2020, The trilobite *Redlichia* from the lower Cambrian Emu Bay Shale Konservat-Lagerstätte of South Australia: systematics, ontogeny and soft-part anatomy: *Journal of Systematic Palaeontology*, v. 18, p. 295–334, doi:10.1080/14772019.2019.1605411.
- Hou, X., and Bergström, J., 1997, Arthropods of the Lower Cambrian Chengjiang fauna, southwest China: *Fossils and Strata*, v. 45, p. 1–116.

- Losso, S.R., and Ortega-Hernández, J., 2022, Claspers in the mid-Cambrian *Olenoides serratus* indicate horseshoe crab-like mating in trilobites: *Geology*, v. 50, <https://doi.org/10.1130/G49872.1>
- Hou, J., Hughes, N.C., and Hopkins, M.J., 2021, The trilobite upper limb branch is a well-developed gill: *Science Advances*, v. 7, p. 1–8, doi:10.1126/sciadv.abe7377.
- Hu, C.-H., 1971, Ontogeny and sexual dimorphism of Lower Paleozoic Trilobita: *Palaeontographica Americana*, v. 7, p. 31–155.
- Laibl, L., Esteve, J., and Fatka, O., 2017, Giant postembryonic stages of *Hydrocephalus* and *Eccaparadoxides* and the origin of lecithotrophy in Cambrian trilobites: *Palaeogeography, Palaeoclimatology, Palaeoecology*, v. 470, p. 109–115, doi:10.1016/j.palaeo.2017.01.023.
- Maruzzo, D., Bonato, L., Brena, C., Fusco, G., and Minelli, A., 2005, Appendage loss and regeneration in arthropods: A comparative view, *in* Koenemann, S. and Jenner, R. eds., *Crustacea and Arthropod Relationships*, CRC Press, p. 225–256, doi:10.1201/9781420037548-17.
- Maruzzo, D., and Bortolin, F., 2013, Arthropod Regeneration, *in* *Arthropod Biology and Evolution: Molecules, Development, Morphology*, p. 149–169, doi:10.1007/978-3-642-36160-9_7.
- McNamara, K.J., and Tuura, M.E., 2011, Evidence for segment polarity during regeneration in the Devonian Asteropygine trilobite “*Greenops widderensis*”: *Journal of Paleontology*, v. 85, p. 106–110.
- Nakamura, T., Mito, T., Bando, T., Ohuchi, H., and Noji, S., 2008, Dissecting insect leg regeneration through RNA interference.: *Cellular and molecular life sciences: CMLS*, v. 65, p. 64–72.
- Ortega-Hernández, J., and Brena, C., 2012, Ancestral patterning of tergite formation in a centipede suggests derived mode of trunk segmentation in trilobites (P. K. Dearden, Ed.): *PLoS ONE*, v. 7, p. e52623, doi:10.1371/journal.pone.0052623.
- Ou, Q., Vannier, J., Yang, X., Chen, A., Mai, H., Shu, D., Han, J., Fu, D., Wang, R., and Mayer, G., 2020, Evolutionary trade-off in reproduction of Cambrian arthropods: *Science Advances*, v. 6, p. eaaz3376, doi:10.1126/sciadv.aaz3376.
- Pates, S., Bicknell, R.D.C., Daley, A.C., and Zamora, S., 2017, Quantitative analysis of repaired and unrepaired damage to trilobites from the Cambrian (Stage 4, Drumian) Iberian Chains, NE Spain: *PALAIOS*, v. 32, p. 750–761, doi:10.2110/palo.2017.055.
- Poschmann, M., and Dunlop, J.A., 2006, A New Sea Spider (arthropoda: Pycnogonida) with a flagelliform telson from the Lower Devonian Hunsrück Slate, Germany: *Palaeontology*, v. 49, p. 983–989, doi:10.1111/j.1475-4983.2006.00583.x.
- Rosin, R., 1964, On regeneration in scorpions: *Israel Journal of Zoology*, v. 13, p. 177–183, doi:DOI: 10.1080/00212210.1964.10688199.
- Schmidt, M., Hou, X., Zhai, D., Mai, H., Belojević, J., Chen, X., Melzer, R.R., Ortega-Hernández, J., and Liu, Y., 2022, Before trilobite legs: *Pygmaclypeatus daziensis* reconsidered

Losso, S.R., and Ortega-Hernández, J., 2022, Claspers in the mid-Cambrian *Olenoides serratus* indicate horseshoe crab-like mating in trilobites: *Geology*, v. 50, <https://doi.org/10.1130/G49872.1>

and the ancestral appendicular organization of Cambrian arthropods: *Philosophical Transactions B*, v. 377, 20210030, <https://doi.org/10.1098/rstb.2021.0030>.

Seifert, A.W., Monaghan, J.R., Smith, M.D., Pasch, B., Stier, A.C., Michonneau, F., and Maden, M., 2012, The influence of fundamental traits on mechanisms controlling appendage regeneration: *Biological Reviews*, v. 87, p. 330–345, doi:10.1111/j.1469-185X.2011.00199.x.

Shaw, V.K., and Bryant, P.J., 1974, Regeneration of appendages in the large milkweed bug, *Oncopeltus fasciatus*: *Journal of Insect Physiology*, v. 20, p. 1849–1857, doi:10.1016/0022-1910(74)90214-5.

Sigvardt, Z.M.S., and Olesen, J., 2014, Mating Behaviour in Laevicaudatan Clam Shrimp (Crustacea, Branchiopoda) and Functional Morphology of Male Claspers in a Phylogenetic Context: A Video-Based Analysis (A. Hejnol, Ed.): *PLoS ONE*, v. 9, p. e84021, doi:10.1371/journal.pone.0084021.

Siveter, D.J., Fortey, R.A., Briggs, D.E.G., Siveter, D.J., and Sutton, M.D., 2021, The first Silurian trilobite with three-dimensionally preserved soft parts reveals novel appendage morphology (X. Zhang, Ed.): *Papers in Palaeontology*, p. spp2.1401, doi:10.1002/spp2.1401.

Wanninger, A. (Ed.), 2015, “Crustacea”: Decapoda (Dendrobranchiata), *in* *Evolutionary Developmental Biology of Invertebrates 4*, Vienna, Springer Vienna, doi:10.1007/978-3-7091-1853-5.

Wills, M.A., Briggs, D.E.G., and Fortey, R.A., 1998, Evolutionary correlates of arthropod tagmosis: scrambled legs, *in* Fortey, R.A. and Thomas, R.H. eds., *Arthropod Relationships*, Dordrecht, Springer Netherlands, p. 57–65, doi:10.1007/978-94-011-4904-4_6.

Wilmot, N.V., 1989, Original mineralogy of trilobite exoskeletons: *Palaeontology*, v. 32, p. 297–304.

Zeng, H., Zhao, F., Yin, Z., and Zhu, M., 2017, Appendages of an early Cambrian metadoxidid trilobite from Yunnan, SW China support mandibulate affinities of trilobites and arthropods: *Geological Magazine*, v. 154, p. 1306–1328, doi:10.1017/S0016756817000279.

Zhai, D., Edgecombe, G.D., Bond, A.D., Mai, H., Hou, X., and Liu, Y., 2019, Fine-scale appendage structure of the Cambrian trilobitomorph *Naraoia spinosa* and its ontogenetic and ecological implications: *Proceedings of the Royal Society B: Biological Sciences*, v. 286, p. 20192371, doi:10.1098/rspb.2019.2371.